



Published in final edited form as:

Nature. ; 475(7357): 510–513. doi:10.1038/nature10183.

Transforming binding affinities from 3D to 2D with application to cadherin clustering

Yinghao Wu^{a,b,d}, Jeremie Vendome^{a,b,d}, Lawrence Shapiro^{a,c,1}, Avinoam Ben-Shaul^{e,1}, and Barry Honig^{a,b,d,1}

^aDepartment of Biochemistry and Molecular Biophysics, Columbia University, New York, NY 10032

^bHoward Hughes Medical Institute, Columbia University, New York, NY 10032

^cEdward S. Harkness Eye Institute, Columbia University, New York, NY 10032

^dCenter for Computational Biology and Bioinformatics, Columbia University, Room 815, 1130 St. Nicholas Avenue, New York, NY, 10032

^eInstitute of Chemistry and the Fritz Haber Research Center, The Hebrew University, Jerusalem 91904, Israel

Abstract

Membrane-bound receptors often form large assemblies resulting from binding to soluble ligands, cell-surface molecules on other cells, and extracellular matrix proteins¹. For example, the association of membrane proteins with proteins on different cells (*trans* interactions) can drive the oligomerization of proteins on the same cell (*cis* interactions)². A central problem in understanding the molecular basis of such phenomena is that equilibrium constants are generally measured in three-dimensional (3D) solution and are thus difficult to relate to the two-dimensional (2D) environment of a membrane surface. Here we present a theoretical treatment that converts 3D to 2D affinities accounting directly for the structure and dynamics of the membrane-bound molecules. Using a multi-scale simulation approach we apply the theory to explain the formation of ordered junction-like clusters by classical cadherin adhesion proteins. The approach includes atomic-scale molecular dynamics simulations to determine inter-domain flexibility, Monte-Carlo simulations of multi-domain motion, and lattice simulations of junction formation³. A finding of

Users may view, print, copy, download and text and data-mine the content in such documents, for the purposes of academic research, subject always to the full Conditions of use: http://www.nature.com/authors/editorial_policies/license.html#terms

¹Correspondence and requests for materials should be addressed to: Barry Honig, Phone: (212) 851-4651, Fax: (212) 851-4650, bh6@columbia.edu; Avinoam Ben-Shaul, Phone: (972)-2-6585271, Fax: (972)-2-6513742, abs@fh.huji.ac.il; Lawrence Shapiro, Phone: (212) 342-6029, Fax: (212) 342-6026, lss8@columbia.edu.

Full methods are available in the online version of the paper at www.nature.com/nature

Supplementary Information is linked to the online version of the paper at www.nature.com/nature.

Author Contributions: Y.W., J.V., L.S., B.H., and A.B.-S. designed research; Y.W. performed research; J.V. carried out the all atom MD simulations; Y.W., B.H., and A.B.-S. analyzed data; Y.W., A.B.-S. and B.H. contributed analytic tools; and Y.W., L.S., B.H., and A.B.-S. wrote the paper.

Reprints and permissions information is available at www.nature.com/reprints.

The authors declare no competing financial interests.

general relevance is that changes in inter-domain motion upon *trans* binding plays a crucial role in driving the lateral, *cis*, clustering of adhesion receptors.

It is commonplace to quantitatively characterize binding between macromolecules by measuring dissociation constants in solution, $K_d^{(3D)}$, which are typically defined in 3D concentration units (e.g. moles/liter). However, phenomena that take place on membrane surfaces are dependent on 2D densities and the relevant dissociation constants, $K_d^{(2D)}$, are defined in units such as molecules/ μm^2 . Measurements of $K_d^{(2D)}$ are difficult to perform and have only been carried out in a small number of cases⁴⁻⁵. Thus, it would be extremely valuable to have a method available that could transform measured values for $K_d^{(3D)}$ into corresponding values of $K_d^{(2D)}$. A reasonable simplifying assumption in such a method is that the binding interface formed by any two molecules is essentially identical in 3D and in 2D. The difference in the K_d s then results only from the change in dimensionality and from any other effects that arise from the constrained environment of a planar system.

Bell and coworkers⁶⁻⁷ transformed between two and three dimensions through the simple expression, $K_d^{(2D)} = h \times K_d^{(3D)}$, where h is the “confinement length”. The basic idea is that if two interacting species are confined to a region h along an axis perpendicular to the plane of a membrane, then they are effectively confined to a volume, Ah , where A is the area per molecule⁶⁻⁸. This simple procedure turns a 2D system into a “quasi-3D system” since there is now a volume associated with each molecule even when it is constrained to a planar membrane. The extent of motion along the third dimension can arise from different factors such as molecular flexibility, rotations with respect to the membrane plane, membrane fluctuations and translational motion of the membranes themselves. A number of studies have used measured 3D and 2D affinities to determine h for individual systems. However, as pointed out by Dustin and coworkers⁵, widely discrepant values have been obtained from the use of different methods to measure 2D affinities; for example fluorescence measurements typically yield values for h on the order of nanometers, whereas mechanical measurements have yielded values for h on the order of micrometers.⁵ Here we focus on cases where two flat parallel membranes are separated by a distance that allows proteins located on opposing surfaces to interact in *trans* and where proteins located on the same surface oligomerize in *cis*. The values of h that we find are on the order of nanometers as is consistent with fluorescence measurements of 2D affinities⁵.

Our specific focus is on the formation of ordered structures by the type I family of classical cadherins. Cadherins have five extracellular immunoglobulin-fold EC domains but the *trans* binding interface is localized entirely on the membrane-distal EC1 domain⁹. We have recently shown that a molecular layer seen in crystal structures of classical cadherins corresponds to the extracellular structure of adherens junctions¹⁰. In addition to the *trans* interface a second, *cis*, interface is formed between the EC1 domain of one cadherin and a region comprising parts of the EC2 and EC3 domains of another (Figure 1). *Trans* cadherin binding affinities have been measured in 3D solution¹¹ while *cis* interactions are too weak to measure but have an upper limit of about 1 mM¹⁰. We use this well-defined system as a

basis for the development of general theoretical expressions that accomplish the transformation from 3D to 2D. These expressions, when used in conjunction with experimental data and our multi-scale simulations, provide a detailed description of the structural and energetic basis of junction formation and elucidate new principles that are likely to be relevant to other systems.

Figure 2(a) describes the *trans* dimerization reaction when cadherins are restricted to the membrane surface. As mentioned above, we assume that the binding interfaces are the same in solution and on a membrane surface so that the *energetic contributions to binding are identical*. $E(3D) = E(2D)$ Hence, the difference in the binding affinities is *entirely entropic*. Since the *trans* dimerization interface is located on EC1, the difference between 3D and 2D affinities is related to the probability that two EC1 domains will encounter one another in an orientation that allows binding. This in turn depends on the local concentration of EC1 domains and on their freedom of rotational motion. As indicated in the figure, we use h_M and h_T to denote the range of EC1 motion normal to the membrane plane corresponding to monomeric and *trans* dimeric cadherins, respectively. Thus, as opposed to Bell's expression⁶⁻⁷ we allow for different values of the confinement length between monomer and dimer, and hence their local concentrations, a factor that will prove crucial in the discussion below. To calculate h_M and h_T we make the simplifying assumption that the two adhering membranes are flat and parallel to each other, as illustrated schematically in Figure 2. Assuming a cadherin density of 80 molecules per square micrometer¹¹ the lateral intermolecular distance is about 100 nm (which becomes much smaller once clustering begins). Estimates based on bending rigidity suggest that, over this lateral distance range, spontaneous fluctuations in membrane height are typically only a fraction of a nanometer¹²⁻¹³, significantly less than the variations in h due to molecular flexibility considered in this work. Of course cells *in-vivo* can extend membranous protrusions such as filopodia, which at some scale are not flat. Consideration of such issues goes beyond the scope of the current work, however the treatment given here should provide a good starting point for these more complex instances.

The factors that enter into our treatment of rotational motion are shown in Figure 2(b), where the orientation of the EC1 binding site is described in terms of the three Euler angles, φ , θ and ψ . In 3D, all three rotational angles are unrestricted. In contrast, there are restrictions on the rotational freedom of the membrane bound molecules, except for the angle φ which corresponds to motion around the z axis. The rotational entropy is related to the integral over the three Euler angles¹⁴, φ , θ and ψ , which yields $8\pi^2$ in 3D and a value, $\Omega < 8\pi^2$, for membrane bound molecules (see Supplemental material). Here, $\Omega = (\omega_M)^2 / \omega_T$ where $\omega_M = 2\pi \psi_M(1 - \cos \theta_M)$ and $\omega_T = 2\pi \psi_T(1 - \cos \theta_T)$ are the “rotational phase space volumes” of monomer and *trans* dimer, respectively (see Supplemental Information for details). In parallel to the confinement lengths h_M and h_T , ω_M and ω_T describe the “confinement” in rotational motion in the constrained environment of the membrane.

In Supplemental Information we derive the expression:

$$\frac{K_d^{(2D)}(trans)}{K_d^{(3D)}(trans)} = \frac{\Omega}{8\pi^2} \times \frac{h_M^2}{h_T} = \frac{1}{8\pi^2} \times \frac{(\Delta\omega_M h_M)^2}{\Delta\omega_T h_T} \quad (1)$$

Equation 1 is quite general although, as presented here, the variables refer specifically to the EC1 domains of cadherins. Note that it is straightforward to transform from 3D to 2D if h_M , h_T , θ_M , ψ_M , θ_T and ψ_T are known. These geometric variables will depend on the structures and flexibility of the proteins involved and on the constraints imposed by the membrane environment.

It is instructive to consider the special, hypothetical, case where the reactive EC1s of monomers and dimers can freely diffuse within the same (“reaction”) volume, so that $h_M = h_T \equiv h$ and, in addition, monomer and dimer rotations in 2D are totally unrestricted, as in 3D ($\Omega/8\pi^2 = 1$). In this case Equation 1 simply reduces to Bell's expression⁶⁻⁷ which, however, does not account for real differences in binding free energies in 2D and 3D. Real differences are due to two effects: (i) Because $h_M > h_T$ and $\omega_M > \omega_T$, the volume available to monomers in 2D is larger than that available to trans dimers, implying a smaller binding affinity as compared to the 3D case. (ii). The rotational entropy loss upon binding in 2D is smaller than that in 3D, as quantitatively represented by $\Omega/8\pi^2 < 1$, resulting in enhancement of the binding affinity in 2D as compared to 3D. These two effects will thus partly compensate each other, as demonstrated below in quantitative terms based on molecular level simulations.

As mentioned above, many membrane receptors form lateral clusters on the cell surface driven by the formation of a distinct inter-protein *cis* interface², which for the specific case of cadherins has been characterized crystallographically^{10,15}. Asymmetric *cis* interfaces can form between two monomers, as well as between two *trans* dimers, as shown in Figure 1. In Supplemental Information we derive equations for the 2D dissociation constants appropriate to the *cis* dimerization of cadherin monomers, $K_d^{(2D)}_{MM}(cis)$ and *trans* dimers, $K_d^{(2D)}_{TT}(cis)$. We show there that

$$\frac{K_d^{(2D)}_{MM}(cis)}{K_d^{(2D)}_{TT}(cis)} = \left(\frac{\Delta\omega_M h_M}{\Delta\omega_T h_T} \right)^2 \quad (2)$$

Equation 2, which accounts for differences in the strength of *cis* interactions between monomers and *trans* dimers, provides physical insights as to the coupling between *trans* and *cis* interactions. Even if *cis* dimers formed from *trans* dimers have an identical interface to that formed between monomers, the affinities will be different due to differences in their respective rotational and vibrational flexibilities, as reflected by the factors ω_M/ω_T and h_M/h_T , respectively. Qualitatively, since both factors are larger than unity, it follows that the lateral attraction between *trans* dimers is stronger than that between monomers.

In Methods we describe a multi-scale simulation approach that yields estimates of the six variables h_M , h_T , θ_M , ψ_M , θ_T and ψ_T that define the transformation between 3D and

2D. It is evident from the simulations (see Figure 3) that *trans* and/or *cis* dimer formation places significant constraints on the molecular system. Values of h , θ and ψ are reduced by approximately a factor of 2-3 in going from a monomer to a *trans* or a *cis* dimer (i.e., $h_T < h_M$; $\theta_T < \theta_M$; $\psi_T < \psi_M$), an effect that will tend to weaken binding affinities (Supplemental Table S1). Table S1 also reports 3D and 2D K_d 's for the dimerization reactions occurring in solution and on the membrane. Notably, the values of $K_d^{(2D)}$ for *trans* interactions reported in Table S1 (ranging from 15 to 250 μm^{-2}) for N-cadherin are in the range obtained from measurements on molecules associated with the T cell system^{4-5,16}, while those for E-cadherin are about an order of magnitude weaker due largely to the greater values of $K_d^{(3D)}$.

The most dramatic effect seen in the simulations is the difference in $K_d^{(2D)}$ of 3-5 orders of magnitude for lateral, *cis*, dimerization affinities between monomers vs. *trans* dimers. The increased binding affinity for *trans* dimers has a clear physical explanation. The association of two cadherin monomers into a *cis* dimer places severe constraints on the inter-domain mobility of both ectodomains such that the spread of allowable values of h , θ , and ψ is significantly reduced, thus resulting in a large entropic penalty for dimerization. In contrast, inter-domain mobility is already reduced in *trans* dimers so that the additional entropic penalty associated with the *cis* dimerization of two *trans* dimers is small compared to that between monomers.

We have previously described the process of adherens junction formation as a phase transition between a dilute phase of monomers and *trans* dimers that diffuse over the surface of a cell, and a condensed lattice composed of *trans* dimers, interacting laterally via a well-defined *cis* interface³. Using lattice simulations we showed that the formation of a condensed ordered phase requires *trans* and *cis* interactions of sufficient magnitude. The results of such simulations, using the 2D binding affinities reported in Table S1, illustrate the formation of well-defined lateral clusters (Figure 4). Thus, converting the measured 3D cadherin binding affinities into 2D free energies yields interactions of sufficient strength to drive *trans* dimer formation, and *cis* interactions between *trans* dimers of sufficient strength to drive the formation of ordered clusters of these dimers. That is, the values of $K_d^{(2D)}$ derived here from a combination of experiment, theory and simulations predict that cadherin ectodomains will form junctions, as is observed. In contrast, owing to the one-dimensional nature of *cis* interaction between monomers (see Figure 1), and because of their small magnitude, monomer oligomerization is negligible³.

It is important to note that the treatment we present is based entirely on forces localized to the extracellular region. This is justified for cadherins since junction-like structures form when cytoplasmic regions are deleted^{10,17}. However, as has recently been demonstrated for TCR-MHC interactions, cytoskeletal forces can affect the kinetic and thermodynamic properties of extracellular domains¹⁸. Thus, although we expect cadherin junction formation in vivo to be affected significantly by cytoplasmic involvement, the process is almost certain to depend on the principles of ordered ectodomain assembly uncovered here.

Finally, the concepts and methods introduced in this work should facilitate the analysis of both *trans* and *cis* binding interactions between other flexible membrane-bound molecules. For example, Dustin and coworkers have shown that chimeras of CD48 with two or three additional Ig-like domains are 10 times less efficient in adhesion than wild type, despite sharing the same binding interface with CD2¹⁹. The entropic penalty associated with restricting inter-domain motion as a consequence of *trans* binding provides a simple explanation of these observations and, more generally, offers a mechanism to control binding affinities of membrane-bound receptors that is not available to molecules that are free in solution.

Methods Summary

Monte Carlo simulations are carried out in which cadherins domains, each treated as a rigid body described at the level of C α atoms, are allowed to move with respect to the membrane surface via random changes in the three Euler angles, Φ , Θ and, Ψ , of the EC5 domain and via motions around the dihedral angles in the hinge regions as indicated in Figure 3 Φ ranges over 360°, while Θ and Ψ are restricted to a limited range (0° in one set of simulations 30° in the other). Motions around the flexible linker regions are described with the Elastic Network Model²⁰⁻²¹ which defines normal modes along which inter-domain motion is allowed. The Block Normal Mode approach²¹⁻²² was applied to partition the structure of cadherin ectodomain into five rigid blocks, each corresponding to one EC domain. The six lowest-frequency modes, each of which describes a collective motion of the entire ectodomain, were used to generate alternate conformations. Fluctuations of the distance between the centers of mass were obtained from MD simulations²³ and were used to calibrate the size of the MC steps along the normal modes.

In each MC step, the EC5 domain was allowed to randomly rotate and then the conformation of the whole ectodomain was changed along one of the normal modes starting with the C-cadherin monomer conformation. For *trans* and *cis* dimers, two ectodomains were first placed in conformations generated from the crystal structure of C-cadherin¹⁵ after which MC steps were taken. Two monomers were defined as forming a dimer if the RMSD obtained from a structural superposition was lower than 6 Å, a value determined from MD simulations²³ as preserving the dimer interface. Values of h_M , h_T , θ_M , θ_T , ψ_M and ψ_T were obtained directly from the conformations generated in the MC simulations.

Supplementary Material

Refer to Web version on PubMed Central for supplementary material.

Acknowledgments

This work was supported by National Science Foundation Grant MCB-0918535 (to B.H.) and National Institutes of Health Grant R01 GM062270-07 (to L.S.). The Financial support of the US-Israel Binational Science Foundation (Grant No. 2006-401, to A.B.-S., B.H., and L.S.), and the Archie and Marjorie Sherman chair (to A.B.-S.), is gratefully acknowledged. We thank Professor Erich Sackmann for a very helpful email exchange concerning membrane fluctuations.

References

1. Aplin AE, Howe AK, Juliano RL. Cell adhesion molecules, signal transduction and cell growth. *Curr Opin Cell Biol.* 1999; 11:737–744. [PubMed: 10600702]
2. Aricescu AR, Jones EY. Immunoglobulin superfamily cell adhesion molecules: zippers and signals. *Curr Opin Cell Biol.* 2007; 19:543–550. [PubMed: 17935964]
3. Wu Y, et al. Cooperativity between trans and cis interactions in cadherin-mediated junction formation. *Proc Natl Acad Sci U S A.* 2010; 107:17592–17597. [PubMed: 20876147]
4. Dustin ML, Ferguson LM, Chan PY, Springer TA, Golan DE. Visualization of CD2 interaction with LFA-3 and determination of the two-dimensional dissociation constant for adhesion receptors in a contact area. *J Cell Biol.* 1996; 132:465–474. [PubMed: 8636222]
5. Dustin ML, Bromley SK, Davis MM, Zhu C. Identification of self through two-dimensional chemistry and synapses. *Annu Rev Cell Dev Biol.* 2001; 17:133–157. [PubMed: 11687486]
6. Bell GI. Models for the specific adhesion of cells to cells. *Science.* 1978; 200:618–627. [PubMed: 347575]
7. Bell GI, Dembo M, Bongrand P. Cell adhesion. Competition between nonspecific repulsion and specific bonding. *Biophys J.* 1984; 45:1051–1064. [PubMed: 6743742]
8. Chen CP, Posy S, Ben-Shaul A, Shapiro L, Honig BH. Specificity of cell-cell adhesion by classical cadherins: Critical role for low-affinity dimerization through beta-strand swapping. *Proc Natl Acad Sci U S A.* 2005; 102:8531–8536. [PubMed: 15937105]
9. Patel SD, et al. Type II Cadherin Ectodomain Structures: Implications for Classical Cadherin Specificity. *Cell.* 2006; 124:1255–1268. [PubMed: 16564015]
10. Harrison OJ, et al. The Extracellular Architecture of Adherens Junctions Revealed by Crystal Structures of Type I Cadherins. *Structure.* 2011; 19:244–256. [PubMed: 21300292]
11. Katsamba P, et al. Linking molecular affinity and cellular specificity in cadherin-mediated adhesion. *Proc Natl Acad Sci U S A.* 2009; 106:11594–11599. [PubMed: 19553217]
12. Gov NS, Safran SA. Red blood cell membrane fluctuations and shape controlled by ATP-induced cytoskeletal defects. *Biophys J.* 2005; 88:1859–1874. [PubMed: 15613626]
13. Zilker A, Engelhardt H, Sackmann E. Dynamic reflection interference contrast (RIC-) microscopy: a new method to study surface excitations of cells and to measure membrane bending elastic moduli. *Journal De Physique.* 1987; 48:2139–2151.
14. Hill, TL. *An Introduction to Statistical Thermodynamics.* Dover Publications; 1987.
15. Boggon TJ, et al. C-cadherin ectodomain structure and implications for cell adhesion mechanisms. *Science.* 2002; 296:1308–1313. [PubMed: 11964443]
16. Dustin ML, et al. Low affinity interaction of human or rat T cell adhesion molecule CD2 with its ligand aligns adhering membranes to achieve high physiological affinity. *J Biol Chem.* 1997; 272:30889–30898. [PubMed: 9388235]
17. Hong S, Troyanovsky RB, Troyanovsky SM. Spontaneous assembly and active disassembly balance adherens junction homeostasis. *Proc Natl Acad Sci U S A.* 2010; 107:3528–3533. [PubMed: 20133579]
18. Huppa JB, et al. TCR-peptide-MHC interactions in situ show accelerated kinetics and increased affinity. *Nature.* 2010; 463:963–U143. [PubMed: 20164930]
19. Milstein O, et al. Nanoscale Increases in CD2-CD48-mediated Intermembrane Spacing Decrease Adhesion and Reorganize the Immunological Synapse. *J Biol Chem.* 2008; 283:34414–34422. [PubMed: 18826951]
20. Atilgan AR, et al. Anisotropy of fluctuation dynamics of proteins with an elastic network model. *Biophys J.* 2001; 80:505–515. [PubMed: 11159421]
21. Li GH, Cui Q. A coarse-grained normal mode approach for macromolecules: An efficient implementation and application to Ca²⁺-ATPase. *Biophys J.* 2002; 83:2457–2474. [PubMed: 12414680]
22. Tama F, Gadea FX, Marques O, Sanejouand YH. Building-block approach for determining low-frequency normal modes of macromolecules. *Proteins.* 2000; 41:1–7. [PubMed: 10944387]

23. Van der Spoel D, et al. GROMACS: Fast, flexible, and free. *J Comput Chem.* 2005; 26:1701–1718. [PubMed: 16211538]

Author Manuscript

Author Manuscript

Author Manuscript

Author Manuscript

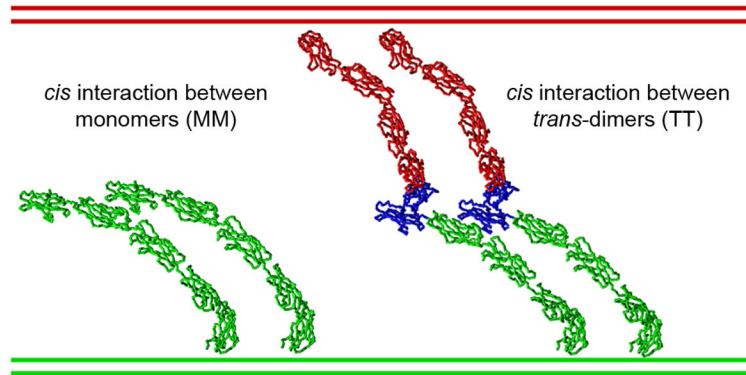


Figure 1. Structures of *cis* dimers formed from cadherin monomers (designated MM) and from *trans* dimers (designated TT)

All coordinates are taken from the crystal structure of C-cadherin ectodomains¹⁵. Note that each TT structure has only a single *cis* interface because the binding regions of the two monomers in a *trans* dimer face in different directions. This property enables the formation of a 2D lattice in which each pair of *trans* dimers makes only a single *cis* interaction^{3,10,15}.

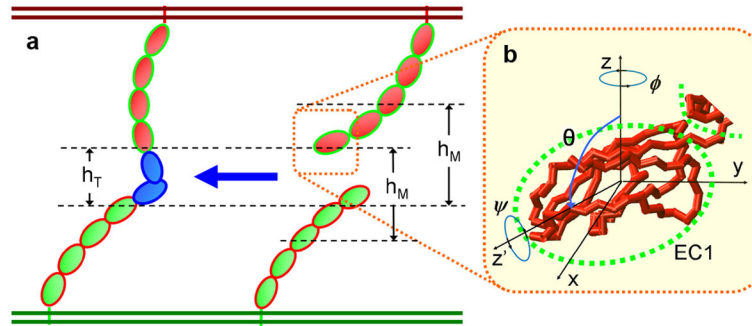


Figure 2. Essential coordinates that characterize the dimerization processes of classical cadherins in a 2D membrane environment

The five domains of cadherin's extracellular regions are represented by ellipsoids. *Trans* dimers (shown in blue) can be formed from two cadherin monomers from two apposing cell surfaces. The molecules are only free to diffuse in two dimensions and rotational motion is constrained. A third dimension is introduced through variations in the perpendicular displacement with respect to the membrane surface, defined by the variable h . h is different for the monomer and *trans* dimer. In general, h_M will be larger than h_T since *trans* binding will limit molecular motion. The rotational degrees of freedom for EC1 domains are characterized by the three Euler angles, ϕ , θ and ψ , as depicted in the right panel.

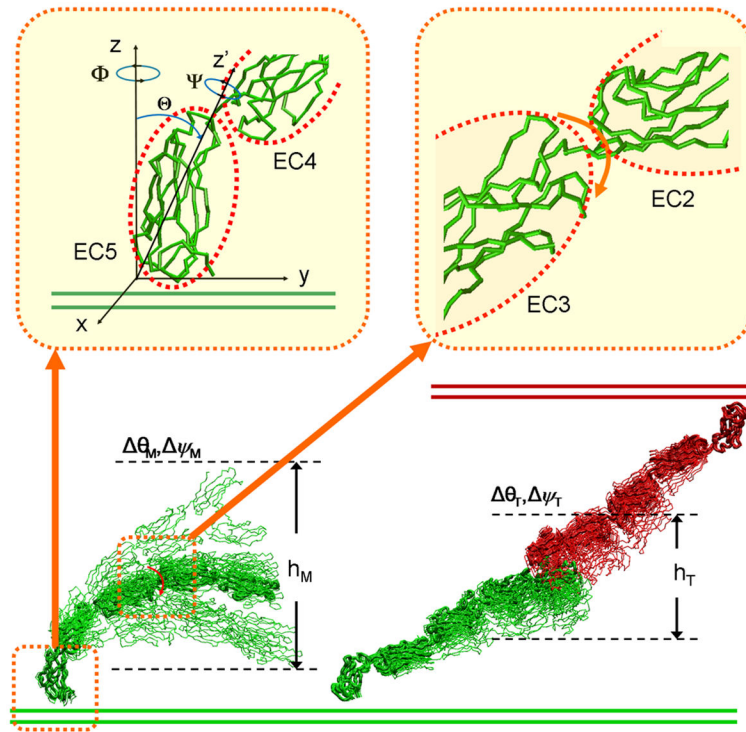


Figure 3. Monte-Carlo simulations of the flexibility of the cadherin ectodomain

The rotations of the EC5 domain with respect to the membrane plane depend on the three Euler angles, Φ , Θ and Ψ of that domain, as shown in the upper left panel. The inter-domain hinge motion indicated by a red arrow is shown in the upper right panel. The lower part of the figure gives the superposition of different conformations in monomer and *trans* dimer generated by the simulations. The range of values for h , ψ and θ can be obtained from the statistical distribution of simulation results. The decreased flexibility of the *trans* dimer with respect to the monomer is evident in the figure. Movies describing molecular motion of the monomers and dimers are included in Supplemental Material.

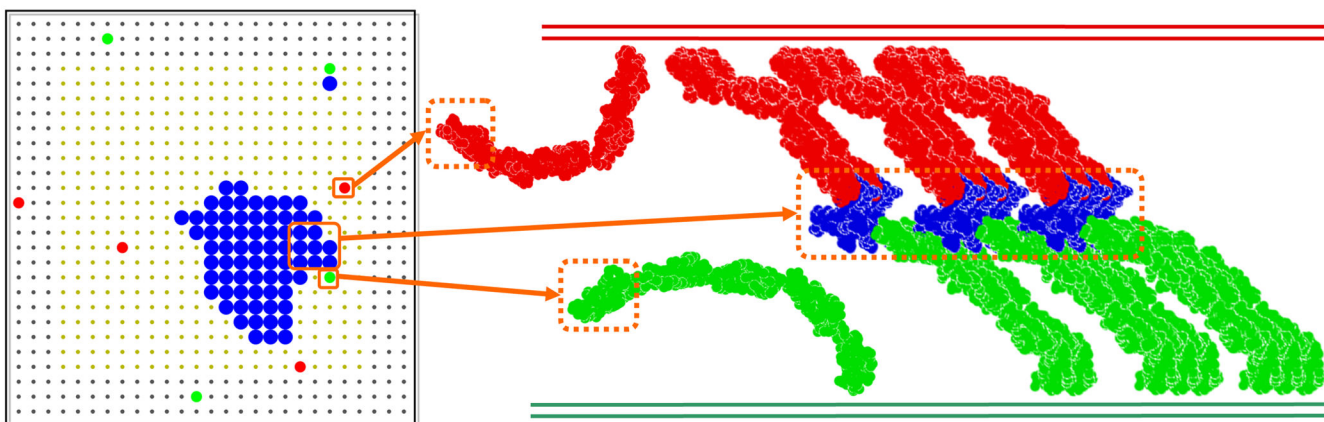


Figure 4. Simulation of junction formation

The lattice in the left panel is a snapshot from a MC simulation where cadherin monomers on apposing cells are colored in red and green, respectively, and *trans* dimers are colored blue³. A diffusion trap mechanism³ in which the trap region comprises 20×20 lattice sites (in yellow), in the center of a 2D lattice of 100×100 sites, with periodic boundary conditions, was used in the simulations. *Trans* dimer formation can only take place in the trap region, as the distance between membranes in the surrounding region is too large to allow *trans* dimer formation. The cadherins form ordered clusters in the trap region, as indicated. Details of the structure appear in reference 10. A movie describing the formation of the ordered junction is included in Supplemental Material. The simulations are carried out using the calculated $K_d^{(2D)}(trans)$ for the *trans* dimerization of E-cadherin (Table S1) that is derived from experimental measurements. The total concentration of monomers in each of the two adhering surfaces (either free or *trans* dimerized) is 1%, while the local concentration in the trap region is much higher (18.5%). The corresponding molecular structures of monomers on both cell surfaces, and part of the cluster formed by eight *trans* dimers are reconstructed in the right panel from the crystal structure of C-cadherin¹⁵ using the same color code. The figure displays the Ca backbone with spheres placed on each carbon atom to improve clarity.